УДК 539.1.074.4

CHERENKOV BEAM COUNTER SYSTEM OF THE CERES/NA45 SPECTROMETER FOR INVESTIGATION WITH 160 GeV/n.LEAD IONS

G.Agakichiev, A.Drees[1], *N.S.Moroz, Yu.A.Panebrattsev, S.V.Razin, N.Saveljic*[2], *S.S.Shimansky, G.P.Škoro*[3], *V.I.Yurevich*

Cherenkov beam counter system of the CERES/NA45 spectrometer was specially designed for experiments with 160 GeV/n lead ions of the SPS CERN. The counters provide a beam monitoring and a realization of a trigger of nucleus-nucleus collision in a target area. Construction scheme and main characteristics of the beam counters and also results of testing with lead beam are presented in this paper.

The investigation has been performed at the Laboratory of High Energies, JINR.

Система черенковских пучковых счетчиков спектрометра CERES/NA45 для исследований с 160 ГэВ/н.ионами свинца

Г.Агакишиев и др.

Система черенковских пучковых счетчиков спектрометра CERES/NA45 была специально разработана для экспериментов с 160 ГэВ/н ионами свинца в ЦЕРН. Счетчики обеспечивают мониторирование пучка и реализацию триггера ядро-ядерного столкновения в области мишени. Представлены конструкция и основные характеристики пучковых счетчиков, а также результаты тестирования на пучке ядер свинца.

Работа выполнена в лаборатории высоких энергий ОИЯИ.

1. Introduction

One of the very important stages of the CERES/NA45 spectrometer modernization, with purpose to prepare and organize experiments with 160 GeV/n Pb-beam, was the elaboration of the beam counter (BC) system which main functions are contained in the following:

1. monitoring of the Pb-beam;
2. selection of the events with nucleus-nucleus collision in the target (interaction trigger);

[1]University of Heidelberg, Germany
[2]University of Montenegro, Yugoslavia
[3]INS «Vinca», Belgrade, Yugoslavia

3. time synchronization of trigger signals and readout of information from the slower main detectors of the spectrometer such as RICH (Ring Imaging Cherenkov) detectors, SIDC (Silicon Drift Chamber) and PC (Pad Chamber);

4. discrimination of the events with more than one Pb projectile within an active time of slower detectors, above mentioned, (before/after protection);

5. operative control of beam passage.

CERES is the experiment dedicated to the measurement of e^+e^- pairs and direct photons in nuclear collisions at SPS energies [1]. From this reason the basic requirement from BC system was minimization of the mass of constructive materials in the beam and target region, which could be potential source of background in measurements. The second, also important, requirement was the stability in the high radiation conditions.

Estimations had shown that for SPS beam structure and intensity of 10^6 nuclei/burst, absorption dose for plastic scintillator of BC would be about 4 Mrad for several days of working. There is well-known fact that for doses above such a value the light output of the scintillator rapidly decreases.

Therefore, BC system needs to provide good time and pulse height resolution and stable working conditions for the long time period (months) for the intensity of $n \cdot 10^6$ nuclei/burst. For realization of these requirements the new system of Cherenkov gaseous detectors, with extremely small mass along the beam path, was designed. Description of the detectors, construction properties, exploitation characteristics and the results of their testing with Pb beam are given bellow.

2. Method

In elaboration of the BC system for the CERES/NA45 spectrometer the following properties of Cherenkov radiation, induced by an ultrarelativistic lead nucleus passing through the gaseous radiator, have been used:

1. Energy of the Pb nucleus is much above the threshold energy for Cherenkov radiation for nitrogen/air radiator, under normal conditions ($E_{th} \simeq 38$ Gev/n);

2. Cherenkov radiation intensity is proportional to the charge squared of the particle and for Pb nucleus ($Z = 82$) there are many photons created per unit length even under the normal pressure;

3. Radiation propagates within a cone with a small angle relative to the beam axis ($\Theta_{max} \simeq 1.38°$ for air under normal conditions) that leads to an opportunity to collect Cherenkov photons, with high efficiency, on photocathode of photomultiplier tube (PMT) even with very small mirror.

The air at normal conditions has been used as a radiator in beam counters. The number of Cherenkov photons per unit length of radiator, within sensitivity range of PMT [λ_1, λ_2], is given by the well-known formula

$$\frac{dN}{dl} = 2\pi Z^2 \alpha \left(\frac{1}{\lambda_1} - \frac{1}{\lambda_2} \right) \cdot \sin^2 \Theta.$$

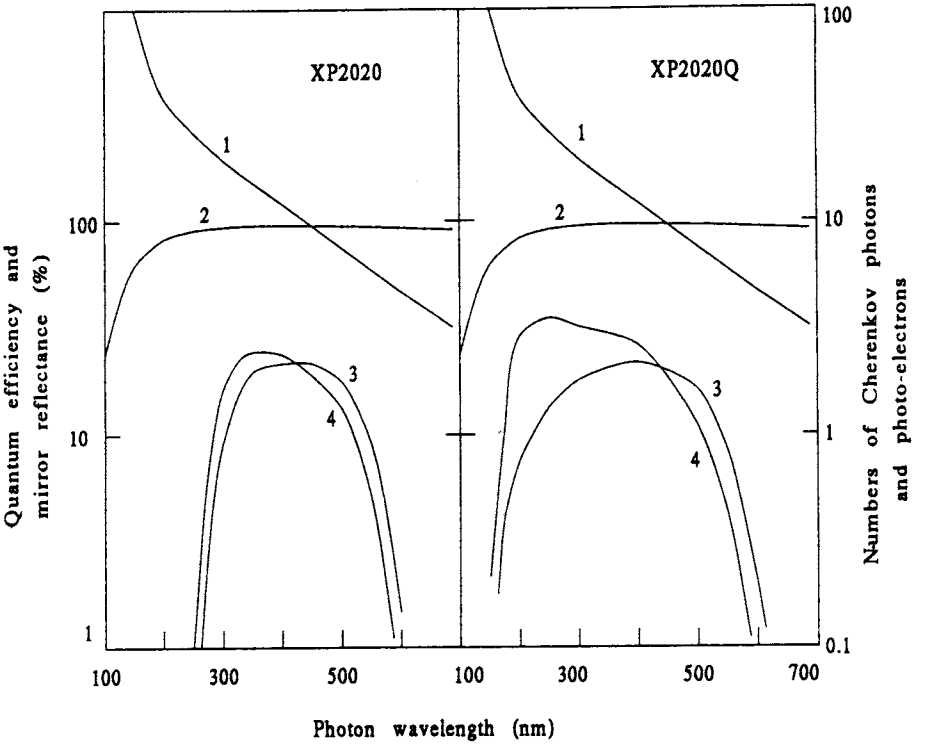

Fig.1. The mean number of photoelectrons versus photon wavelength (1 — number of Cherenkov photons, 2 — mirror reflectance, 3 — quantum efficiency of photocathode, 4 — number of photoelectrons)

Pb nucleus produces $\simeq 2700$ photons along 1 cm of air radiator in wave length interval $\lambda = 300 - 550$ nm and $\simeq 5700$ photons within interval $\lambda = 200 - 550$ nm corresponding to domain of maximum sensitivity of PMT XP2020 and XP2020Q, respectively, which have been used in BC. Figure 1 shows the mean number of photoelectrons versus photon wavelength, for these PMT.

In the case of Pb ion disintegration as a result of its collision with target or surrounding medium nucleus, response of the BC is proportional to the sum of charge squared of the projectile fragments if the distance between produced fragments is longer than the wavelength of Cherenkov radiation.

The layout of beam counters along the beam channel is shown in Fig.2. BC system of the CERES experiment consists of three Cherenkov detectors BC1, BC2, and BC3, and each of them solves its own functional tasks. To avoid upstream interactions as much as possible, a vacuum pipe is used up to the target region. The Cherenkov beam counter, BC1 has been installed in the beam pipe, 60 m upstream of the target. It is responsible for beam monitoring and start signal production by an incident ion. Detector BC2 is situated behind the CERES spectrometer, 6.35 m downstream of the target, and is responsible for detection

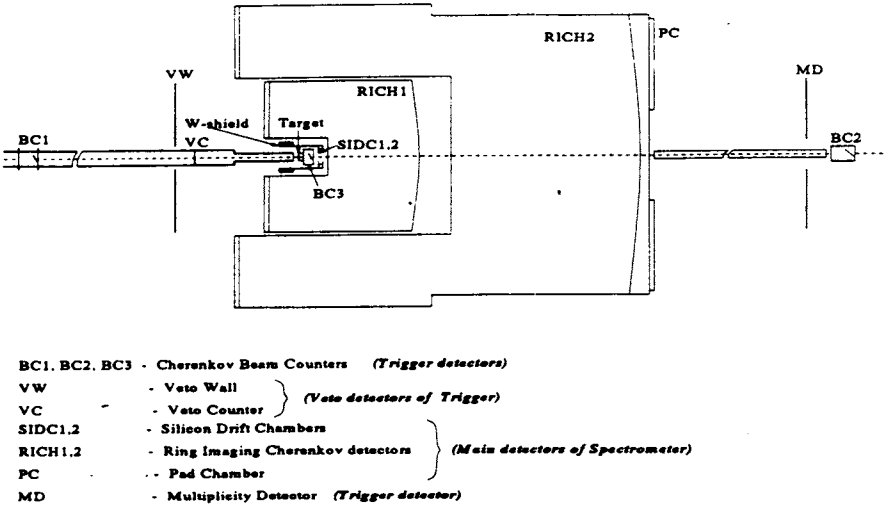

Fig.2. A layout of trigger detectors at the CERES experiment area

of projectiles passing through the experimental apparatus.The Cherenkov micro-counter BC3 is located right behind the target and its basic function is to establish a fact of nucleus-nucleus collision with the absence of Pb nucleus after the target. Interactions downstream of the target but in front of multiplicity detector (MD) cannot be ignored when triggering at low multiplicities. These events can be vetoed by BC3, too. The target is placed at the beam focus with the beam spot diameter of < 600 μm.

Good time characteristics of Cherenkov radiation and PMT XP2020 allow one to organize 10-ns coincidence of signals from BCs, for interaction trigger and also other additional triggers usefull for analysis of the beam passage and searching for background conditions.

Signals from BCs come to the fast discriminator (model 4F115 LHE, JINR) and Ch.ADC (LeCroy VME model 1182). Discrimination thresholds for BC1 and BC2, which have better amplitude resolution than BC3, are set down on the level of about 80% and for BC3 on the level of 50% of the mean pulse heigth of Pb nuclei. After fine adjustment of beam and counter operation we have the following condition for coincidence rates

$$BC1 \cdot BC2 = BC1 \cdot BC3 \cdot BC2$$

Interaction trigger was organized by means of coincidence of the logical signal from BC1 and veto signal from BC3.

So, with these three beam counters there were organized four different types of the simplest triggers:

1. beam trigger — BC1;
2. clear passage of beam ion without disintegration — $BC1 \cdot BC3 \cdot BC2$;
3. interaction trigger — $BC1 \cdot \overline{BC3}$;
4. background interaction behind the target — $BC1 \cdot BC3 \cdot \overline{BC2}$.

Logical signals from BC1, BC2, BC3 and interaction trigger are passed to the inputs of TDC (Le Croy VME model 1172) for off-line controle of the time structure of the signals and organization of B/A protection.

3. Beam Counters

The mirrors of the beam counters were done by vacuum evaporation of 0,999999 Al from the tantalum base on 12 μ mylar with very small heterogeneity over the thickness. The thickness of the settled aluminium layer was 500—800 Å. The factor of reflection measured for $\lambda = 200$ nm was 80%. Construction of Cherenkov counter BC1 is shown in Fig.3. There is no essential difference between the constructions of BC1 and BC2. Entrance window of BC2 was placed parallel with the mirror plane at an angle of 45° to the beam axis with the aim to minimize a path length scattering in radiator for different lead projectiles.

Geometry of the target region and construction of BC3 is shown in Fig.4. Cherenkov light produced in BC3 radiator by projectile is taken out with 2 m optical cable. Light-guide core of the cable has the diameter of 5 mm and consists of thin quartz fibre set with wavelength cut in ultra violet region at $\lambda_{min} = 180$ nm. One end of the cable enters to the radiator chamber of BC3 at angle of 45° and another one is connected with photocathode of PMT XP2020Q.

Before an installation of BC3 a fine tuning of the mirror position was done with special light source producing the light along the BC3 chamber axis. A method of the mirror adjustment was based on requirement to obtain light image around the centre of semi-transparent screen which was placed on the edge of an aluminium tube (entrance of the

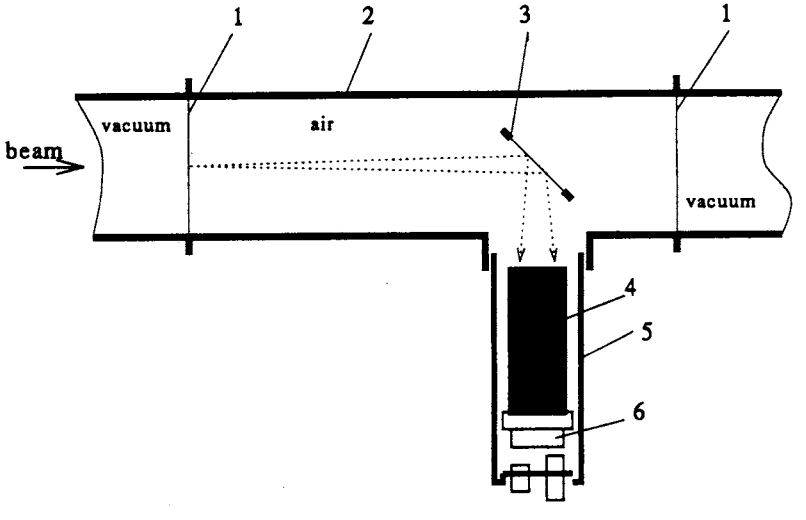

Fig.3. Construction of Cherenkov counter BC1 (1 — mylar windows, 2 —Cherenkov chamber walls, 3 — mirror, 4 — photomultiplier XP2020, 5 — soft iron tube, 6 — voltage divider)

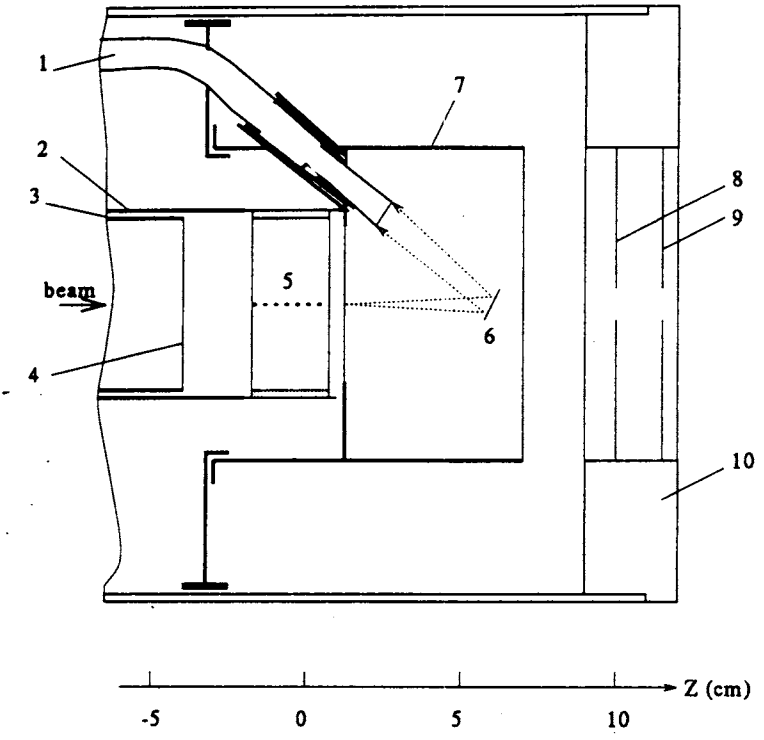

Fig.4. Target area and Cherenkov counter BC3 (1 — optical cable, 2 — carbon pipe, support of the target, 3 — vacuum carbon pipe, 4 — mylar window, 5 — target, 6 — mirror, 7 — Cherenkov chamber of the BC3, 8 — SIDC1, 9 — SIDC2, 10 — SIDC mechanical support)

optical cable into BC3 chamber). The geometry of BC3 was such that a lead nucleus passing through the radiator produces Cherenkov light spot on the polished edge of the optical cable with the lateral dimension less than the diameter of lightguide area. The basic characteristics of beam counters are given in Table 1 and list of constructive materials along the beam path is given in Table 2.

Special investigation has shown that light attenuation factor on the way mirror–optical cable–PMT is 7.5. It leads to the corresponding diminishing in the photoelectrons number on photocathode of PMT and as a consequence to the decreasing of the amplitude resolution relative to the values obtained with BC1 and BC2. The usage of optical cable and PMT with $\lambda_{min} \simeq 180$ nm in BC3 allows one to increase efficiency of Cherenkov radiation detection. Although, the length of radiator in BC3 chamber is rather short and light attenuation factor is rather high, there are $\langle N_e \rangle = 400 \pm 70$ photoelectrons from PMT photocathode created by Pb nucleus passing through the radiator.

Table 1

characteristics	BC1	BC2	BC3
air radiator length (mm)	170	206	43
beam spot			
x direction	± 20 mm	< ± 5 mm	< ± 300 μ
y direction	± 5 mm	< ± 5 mm	< ± 300 μ
mirror			
position from the target	60 m	6.56 m	59 mm
diameter (mm)	63	55	6
frame material	3 mm Al	3 mm Al	1.5 mm rohacel
angle to the beam axis	45°	45°	22.5°
PMT			
type	XP2020	XP2020	XP2020Q
λ range (nm)	300—550	300—550	200—550
rise time (ns)	1.5	1.5	1.5
pulse height resolution	7%	7%	7%
photocathode ∅ (mm)	42	42	42

Table 2

Beam counter	Material	Thickness
BC1	mylar window 1	100 μ
	air	270 mm
	mylar mirror	17 μ
	mylar window 2	100 μ
BC2	black paper window 1	140 μ
	air	240 mm
	mylar mirror	17 μ
	black paper window 2	100 μ
BC3	black paper window 1	100 μ
	air	50 mm
	mylar mirror	13 μ
	black paper window 2	100 μ

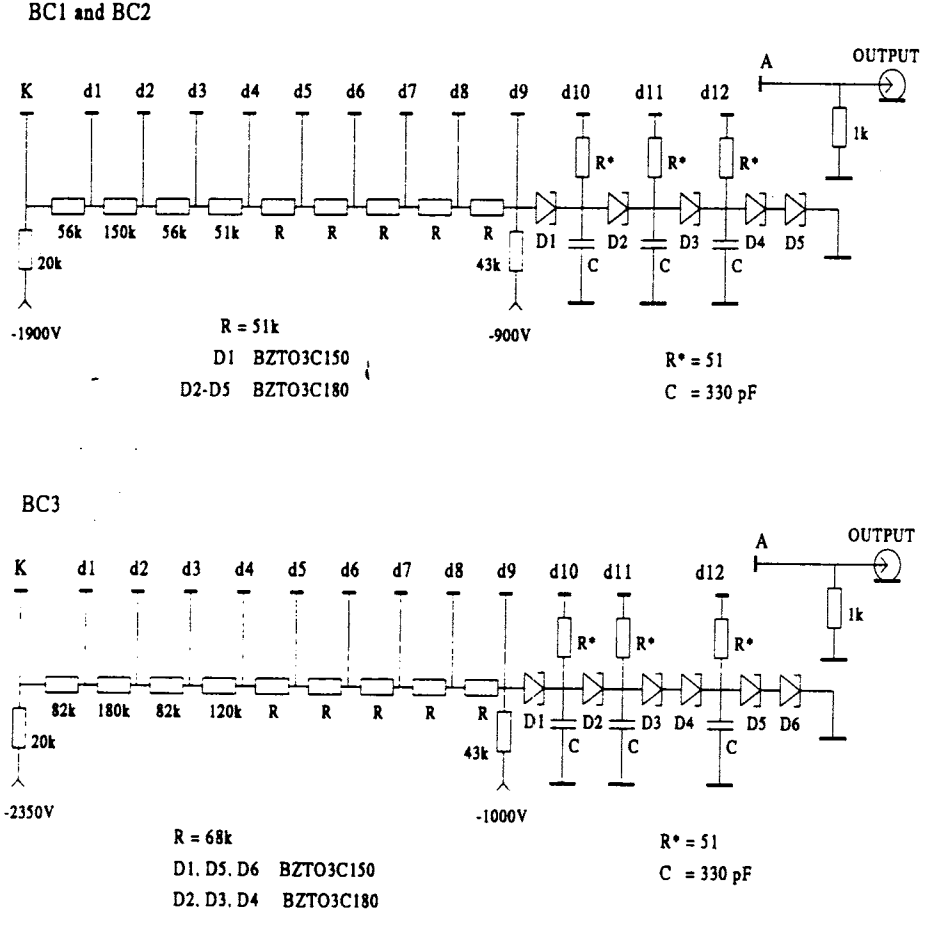

Fig.5. Voltage dividers of photomultipliers of the beam counters

To get a stable operation of PMT for high intensity of beam the voltage for last dynodes was created with a chain of diodes BZTO3C150, 180 and additional high voltage power supply. Scheme of the voltage divider is shown in Fig.5. Beam counters were supplied from the Le Croy high voltage multichannel system.

4. Beam Test

The first experience of the new BC system application in the level 1 trigger of the CERES experiment was performed with 160 GeV/n Pb beam in November/December 1995. The intensity of beam was about $5 \cdot 10^5$ ions/burst.

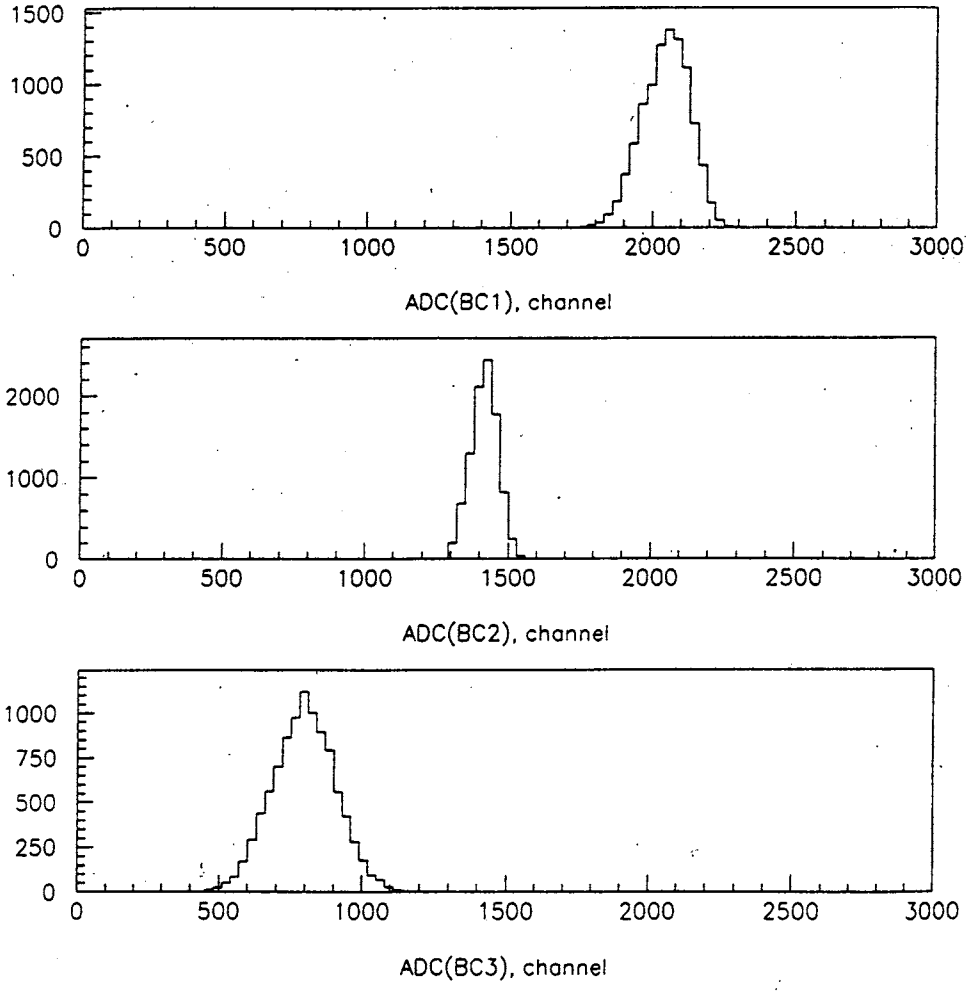

Fig.6. Responses of the beam counters for lead ions

4.1. Beam Counter Operation. An analysis of the operation characteristics of the counters showed the stable working capabilities of each beam counter during 25 days run. Study of the detector responses and the trigger operation during the run '95 was done with the special runs using the two simplest triggers: interaction trigger (trigger 3) and beam trigger (trigger 1). Taking into account the ADC and TDC information obtained with beam counters one can organize the additional triggers (2) and (4) mentioned above for the off-line analysis of clear passage of lead ions and background interactions. All beam counters had good responses for lead ions with the Gaussian shape of peak (relative uncertainty of ~4% for BC1 and BC2 and ~14% for BC3). The BC responses for lead ion obtained with trigger (2) are presented in Fig.6.

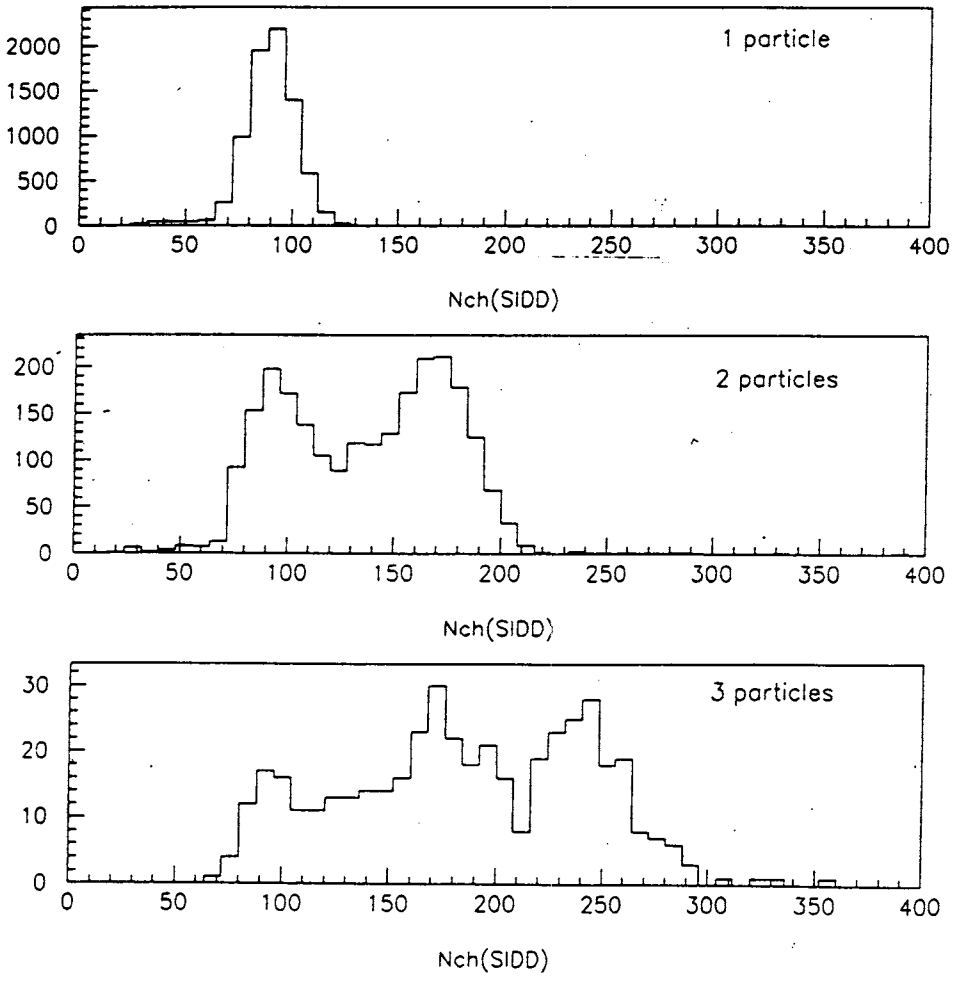

Fig.7. The response of the SIDC1 for one, two and three lead ions passing the target area without interaction within a time interval ± 5 μs

4.2. Before/after Protection. For the main detectors of the CERES spectrometer the background contribution to the detector response produced by pile-up of ions was analysed using the TDC information on a beam position on a time scaler obtained with beam counters. For this purpose trigger (2) was used for selection of the clear passage of lead ions through the experimental area. Under this condition, the background response of the SIDC is mainly produced by δ-electrons. Some additional number of hits appeared if more than one ion has passed through during the active time of the SIDC. The SIDC responses for three cases (1, 2 and 3 ions within the time interval ± 5 μs) are shown in Fig.7. The result is a rise of background with increasing a number of ions per active time of the detector. More clear information on the dependence of the number of background hits on

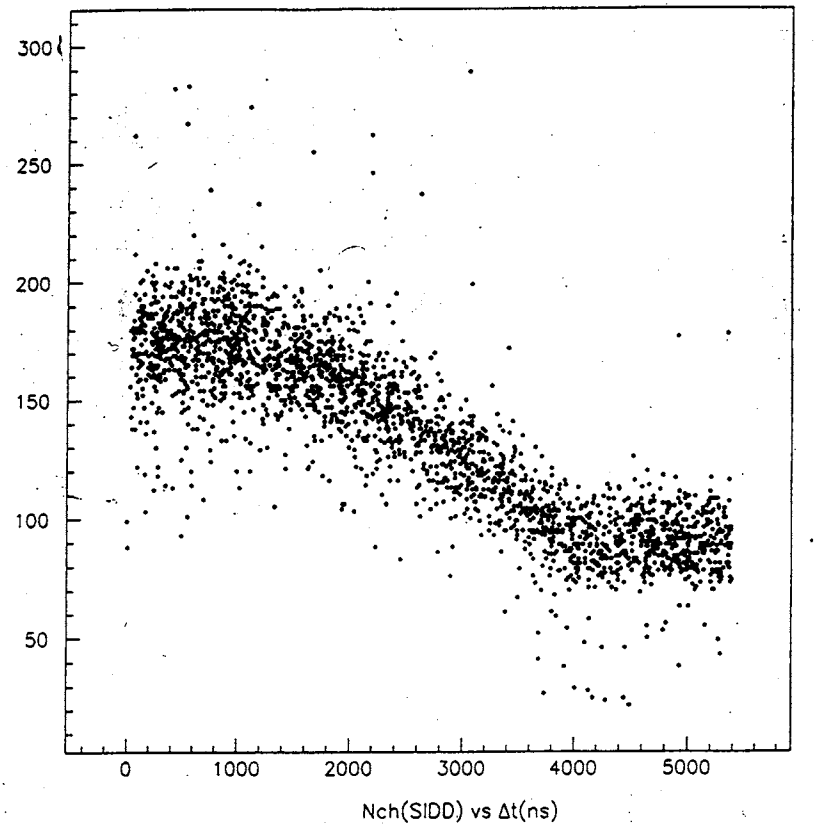

Fig.8. A background hit contribution to the SIDC1 response as a function of time interval between two lead ions passing the target area without interaction

the time distance between two ions is presented in Fig.8. One can see that the hits number increases from ~90 (one ion in the active time of the SIDC) to ~180 (two ions with a small time discrepancy) within the time interval ± 4 μs corresponding to the active time of the SIDC. This effect can be the main limitation in a way to work with a high intensity of beam.

4.3. Interaction Trigger. The major purpose of the interaction trigger for the CERES/NA45 experiment is an effective selection of Pb-Au collisions in the maximum wide region of impact parameter including closed and peripheral nuclear interactions. The main trigger function is to discriminate the BC3 signals with the pulse height more than threshold value settled as it has been mentioned above. The BC3 and BC2 responses are in a strong dependence on the lead ion fragmentation process and correspond to a sum of charges squared for fragments passing the radiator within the BC acceptance.

The Monte Carlo simulation of the perpendicular momentum distribution of lead ion fragments was estimated according to approach [2] with approximation of fragment charge composition [3]. The simulation results showed that the BC3 acceptance covers all

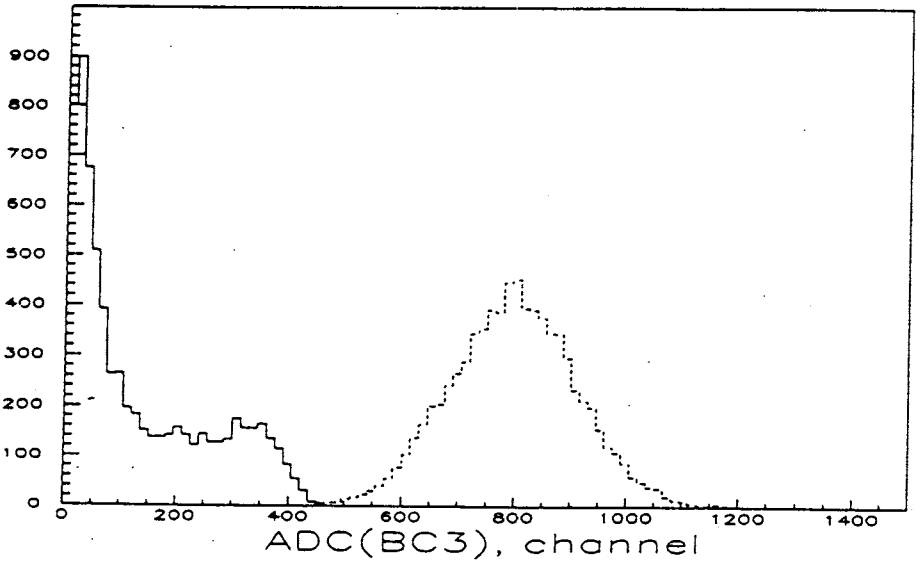

Fig.9. Pulse height distributions for Cherenkov counter BC3. Solid histogram — interaction trigger (3), dashed histogram — trigger (2)

projectile fragmentation region and the BC2 sees all fragments with charge more than 20, and some part of low charged fragments is missed.

The pulse height distributions obtained from the BC3 with two different triggers (2) and (3) are shown in Fig.9. The discrimination threshold was settled just before the peak produced by Pb and Pb-like-nuclei. A contribution of the different sources of lead ion disintegration, with a multiple production of charged particles in the target area selected by the interaction trigger, was studied by the vertex procedure where the interaction point was determined using the information from doublet of tracking devices SIDC1 and SIDC2.

The CERES target consisted of 8 disks with a thickness of 25 μm each and a diameter of 600 μm. They were spaced by 3 mm and a total thickness of target was 200 μm of Au. There were $\simeq 95\%$ of beam ions hitting the target. The largest amount of events concentrates in the target position ($-3 < z < 0$ cm) where all 8 microtargets are well seen separately as one can see in Fig.10. This figure demonstrates the MD response (charged particle multiplicity) versus z-coordinate of the vertex. The contributions from the interactions with mylar window of the vacuum pipe and the entrance window of the BC3 chamber are clearly visible at $z \simeq -5.3$ cm and 0.5 cm, respectively. For the further analysis of Pb-Au collisions we select only interactions with the target. In the frame of geometrical picture the geometrical cross section as a function of the impact parameter can be obtained by the integration over the overlaped region of the two nuclei. For Pb and Au nuclei the nuclear density is about constant and maximum up to radius $R \simeq 5$ fm and then the density falls down fast in a range $5 < R < 8$ fm with increasing of the radius. So the impact parameter $b < b_0 = 10$ fm corresponds to the interaction of two cores having the maximum density

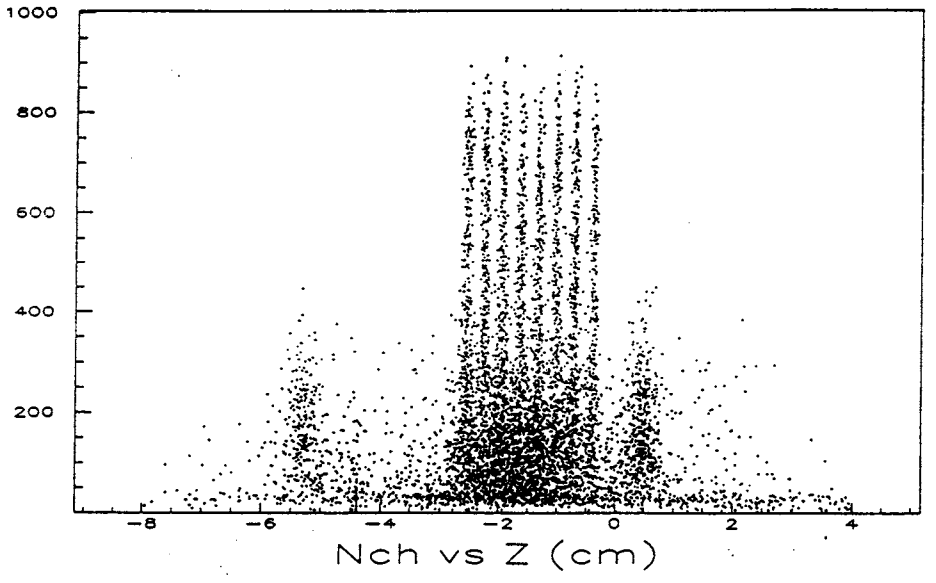

Fig.10. The sources of particle production in the target area presented as a correlation between MD response (number of charged particles, N_{ch}) and z-coordinate obtained by vertex

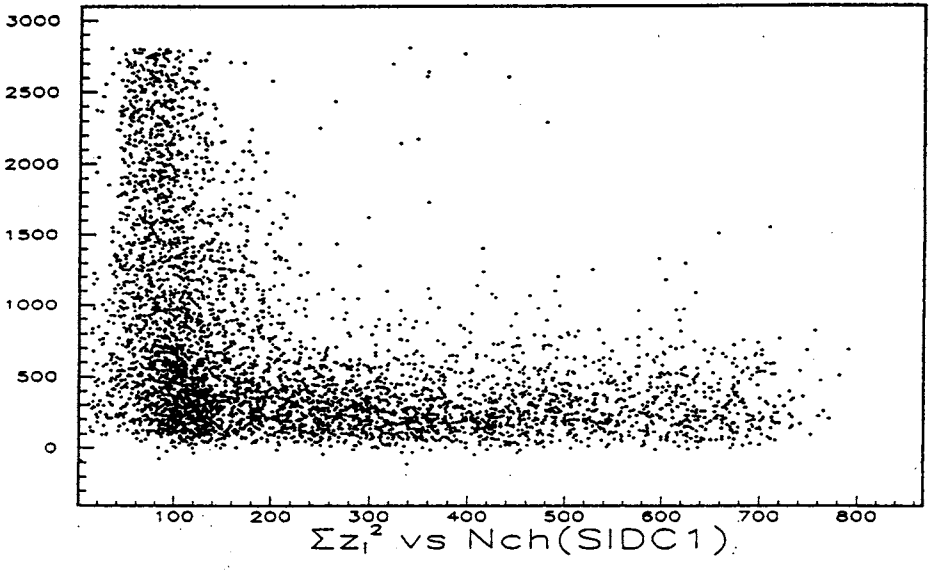

Fig.11. A correlation between the SIDC1 and BC2 responses measured for Pb-Au collisions with the interaction trigger

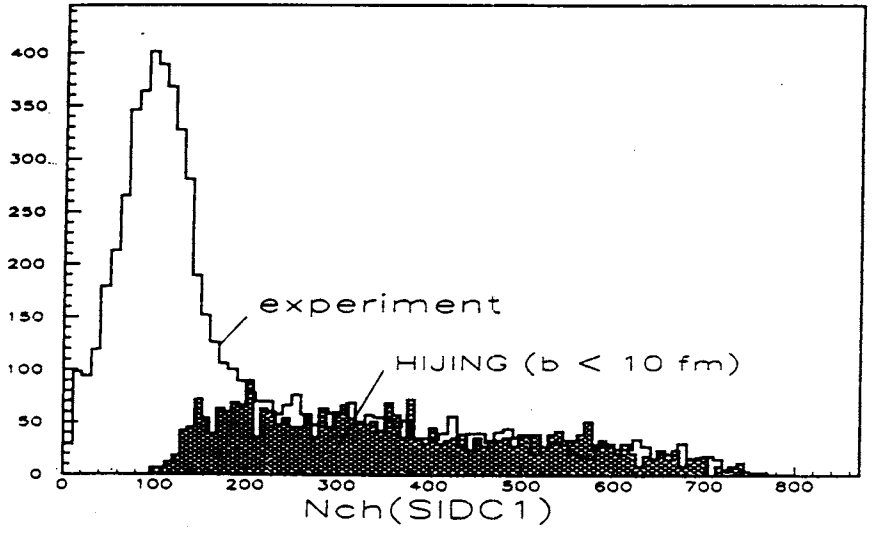

Fig.12. Multiplicity of charged particles produced in Pb-Au collisions within the SIDC acceptance measured with the interaction trigger and predicted by HIJING for $b < 10$ fm

which occurs in central and semicentral collisions. The geometrical cross section for these collisions can be calculated as

$$\sigma_c = \pi b_0^2 = 3.14 \text{ b.}$$

The radius range $5 < r < 8$ fm corresponds to a thickness of low density surface of Pb and Au nuclei and defines in the first approximation the geometrical cross section of Pb-Au peripheral collisions as

$$\sigma_p = \pi \cdot (b_{\max}^2 - b_0^2) = 4.90 \text{ b,}$$

where $b_{\max} = 2 \cdot r_{\max} \simeq 16$ fm.

The experimental study of the trigger efficiency for closed and peripheral Pb-Au collisions was performed by analysis of a correlation between two processes, lead ion fragmentation (BC3 and BC2 responses) and the multiple production of charged hadrons in a midrapidity region corresponding to the maximum yield of secondaries and covered by the SIDC1 ($1.85 < \eta < 3.81$) and the MD ($2.94 < \eta < 4.70$). As an illustration the similar result on a correlation between the BC2 and the SIDC1 data is shown in Fig.11. The BC2 data were transferred to the scale of sum of fragment charges squared by a normalization

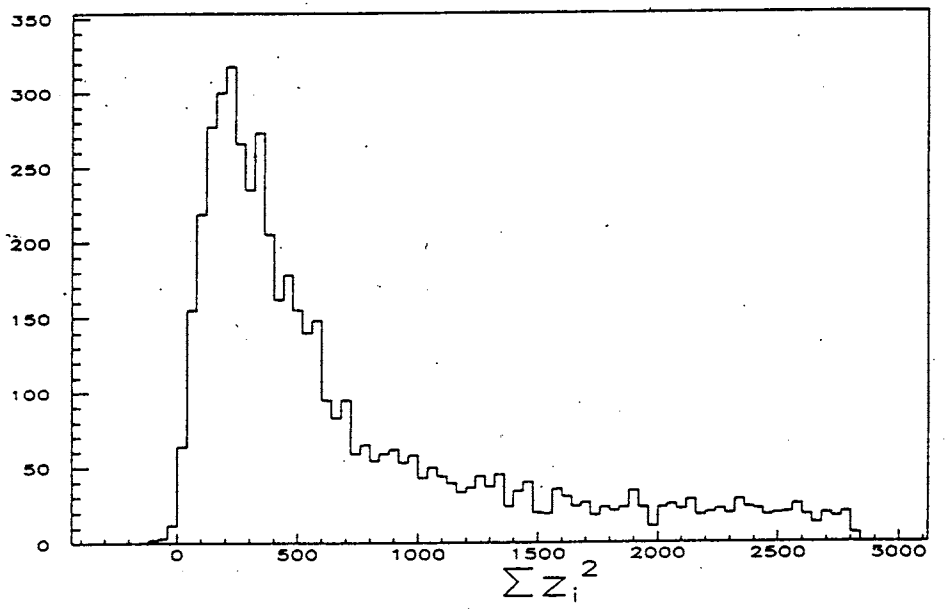

Fig.13. The distribution of sum of fragment charges squared measured for Pb-Au collisions with the interaction trigger

at Pb-ion peak position. The upper limit of the BC2 pulse height was reduced a bit with the aim to expel an influence of BC3 threshold. The large response of BC2 can be observed only for the SIDC multiplicities less than about 150. For the region of multiplicities more than 150, the interaction trigger selects all events without cut. A correspondence between the charged multiplicity within the SIDC1 acceptance and the impact parameter of Pb-Au collisions was investigated with the HIJING event generator [4]. A comparison of the HIJING model prediction for the collisions at $b < 10$ fm with the SIDC1 experimental data is shown in Fig.12. One can see that the HIJING reproduces well the experimental multiplicity data at $b < 10$ fm. The SIDC1 multiplicity of 150 is produced by the nucleus-nucleus collision at impact parameter $b_0 \simeq 10$ fm. The bump in the experimental data at low multiplicities $N_{ch} < 150$ corresponds to nucleus-nucleus collisions with $b > 10$ fm and has a clear and simple explanation taking into account a large geometrical cross section of peripheral collisions.

So the interaction trigger works with the efficiency of $\simeq 100\%$ for semicentral and central collisions. The big dispersion of the Σz_i^2 value in the low multiplicity region due to the event-by-event fluctuation of Pb-ion disintegration in the peripheral collisions is observed and there is a high probability of strong disintegration of Pb nuclei without any high-charged fragments even in the peripheral collisions.

Table 3

Impact parameter region	Z_{max}
$b < 8$ fm	< 25—30
$b < 10$ fm	< 40—$50 \simeq 0.5Z_{Pb}$
$b > 10$ fm	$< 0.5Z_{Pb}$, for the most fraction of events

The upper limits of fragment charge, Z_{max}, for different impact parameter regions estimated on the experimental results are given in Table 3. The pulse height distribution measured by the BC2 with the interaction trigger is presented in Fig.13. The measurements showed that the threshold of the trigger cuts only a small fraction of the nuclear inelastic peripheral collisions. The cross section of peripheral collisions registered can be estimated as

$$\sigma_p^{exp} = \sigma_c \cdot \frac{N_p}{N_c} = 4.35 \text{ b},$$

where N_p and N_c are number of events with N_{ch} (SIDC1) < 150 and > 150, respectively. This experimental value is only a bit less than one obtained above in a frame of geometrical

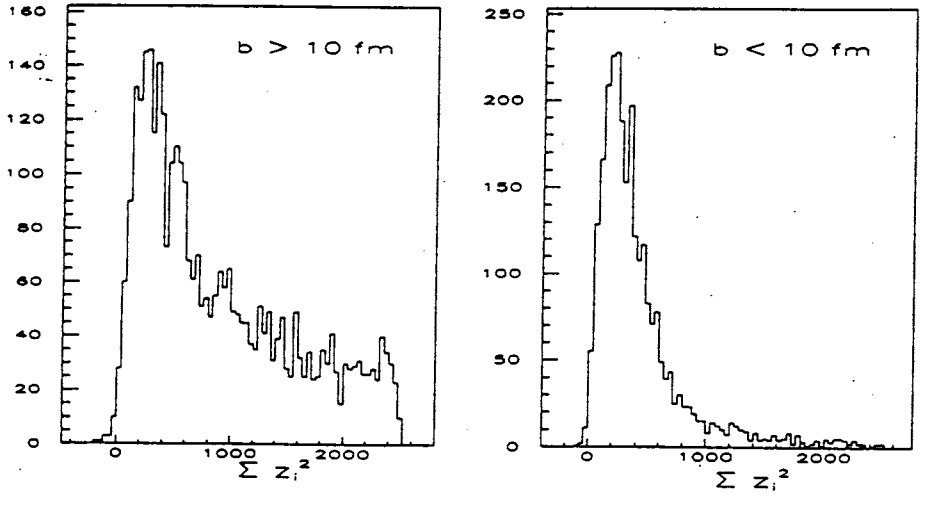

Fig.14. Experimental distributions of a sum of charges squared of lead fragments (BC2 data) for Pb-Au collisions for two impact parameter regions, $b > 10$ fm (left) and $b < 10$ fm (right)

picture of collision. The Σz_i^2 experimental distributions obtained with the BC2 for two cases of Pb-Au collisions with impact parameters $b > 10$ fm ($N_{ch}(\text{SIDC1}) < 150$) and $b < 10$ fm ($N_{ch}(\text{SIDC1}) > 150$) are shown in Fig.14. Here one can see separately the fragmentation of Pb ions in closed and peripheral collisions with Au-nuclei at 160 GeV/n energy and that there are no high-charged fragments at semicentral and central collisions.

We suppose that presented results can be of interest for the trigger design for the central and peripheral nucleus-nucleus collisions study as well as for testing of theoretical models including the description of the projectile nucleus fragmentation at ultrarelativistic energies.

5. Conclusion

The system of Cherenkov gaseous beam counters for monitoring of ultrarelativistic lead ions and an interaction trigger design was developed for the CERES/NA45 experiment in CERN. Test measurements with the lead beam at 160 GeV/n showed that such devices are capable to operate for a long term without any changes of their characteristics. The installation of the beam counters on a beam line led to a very small rise of the background. The analysis of detector responses showed the 100% efficiency of the interaction trigger for semi-central and central collisions of Pb and Au nuclei with low contribution of background interactions with window foils of vacuum pipe and Cherenkov counter chamber, BC3. We intend to continue our work on a development of the beam counter system for the CERES experiment and believe it has a good outlook.

6. Acknowledgements

We would like to thank the members of the CERES collaboration for their help in detector integration into spectrometer scheme. Specially we wish to acknowledge Profs. I.Tserruya, P.Glassel, and P.Wurm for their support of our work and the stimulating discussions.

References

1. CERES/NA45 Report to Cogne 1995, CERN/SPSLC 95-20, 1995.
2. Lepore J.V., Riddel D.J. — Report LBL-3086, 1974.

3. Adamovich M. et al. — Zeitsch. Phys., 1992, v.C55, p.235; Krasnov S.A. et al. — JINR Communications, P1-88-252, Dubna, 1988.
4. Wang X.N., Gyulassy M. — Phys. Rev., 1991, v.D44, p.3501; Phys. Rev., 1992, v.D45, p.844.

Received on December 10, 1996.